

Micro-Raman Spectroscopy of Silica and Hafnia Laser Damage Sites

Ji-Mi Jang

Pittsford Mendon High School

Advisor: **Dr. Tanya Kosc**

Laboratory for Laser Energetics

University of Rochester

Rochester, New York

January, 2020

Abstract

Micro-Raman spectroscopy was used to characterize laser-induced material modification of silica and hafnia thin films, which are used to produce critical multi-layer dielectric thin film coatings for the Omega Laser Facility at the Laboratory for Laser Energetics. Several parameters relevant to laser-induced damage, such as laser fluence, testing protocols (1-on-1 versus N-on-1 tests), and thin film materials have been probed and compared through the analysis of their Raman spectra. The spectra obtained for silica and hafnia thin films are similar, both showing Raman features and photoluminescence (PL), but easily discernible. Clear distinctions in PL intensity help differentiate between low and high fluence damage sites as well as between damaged and undamaged areas. This information could be applied to the future design and manufacturing of thin film coatings.

1. Introduction

Micro-Raman spectroscopy is a non-damaging technique that studies vibrational modes of molecules to analyze molecular interaction and structure. During the process, a laser beam irradiates a test site, and some of the laser energy is absorbed by certain bonds, providing energy to start a vibration between two atoms. The different vibrational modes are specific to certain bonds, allowing the modes to be used as identifying characteristics useful for analyzing molecular structures. Different types of scattering can occur, each resulting in a different wavelength (λ) of the reemitted signal (Figure 1). The first type is Rayleigh scattering, which occurs when none of the laser energy is lost to initiating vibrations, and the reemitted light has the same wavelength as that of the incident beam. The second type is scattering due to the Raman effect, from which, depending on the frequencies of the vibrations, the reemitted

wavelengths differ from the incident laser beam wavelength. The unit (quantum) of energy transferred to atomic or molecular vibrations is referred to as a phonon. The energy of the incident photon that was not transferred to a phonon becomes the energy of the scattered photon and determines the new wavelength of the reemitted light that produces the Raman signal. These new wavelengths are represented by a shift from the wavelength of the incident laser beam and are quantified in terms of the wavenumber shift (cm^{-1}). Wavenumber is a measure of spatial frequency and is defined as $1/\lambda$. Zero wavenumber shifts correspond to the wavelength of the incident (pump) laser beam, so any wavelength deviation indicates a shift in frequency of the reemitted light from the incident beam. Compared to Rayleigh scattering, the Raman effect is much weaker. Nonetheless, it produces essential information that this work uses to investigate material modifications.

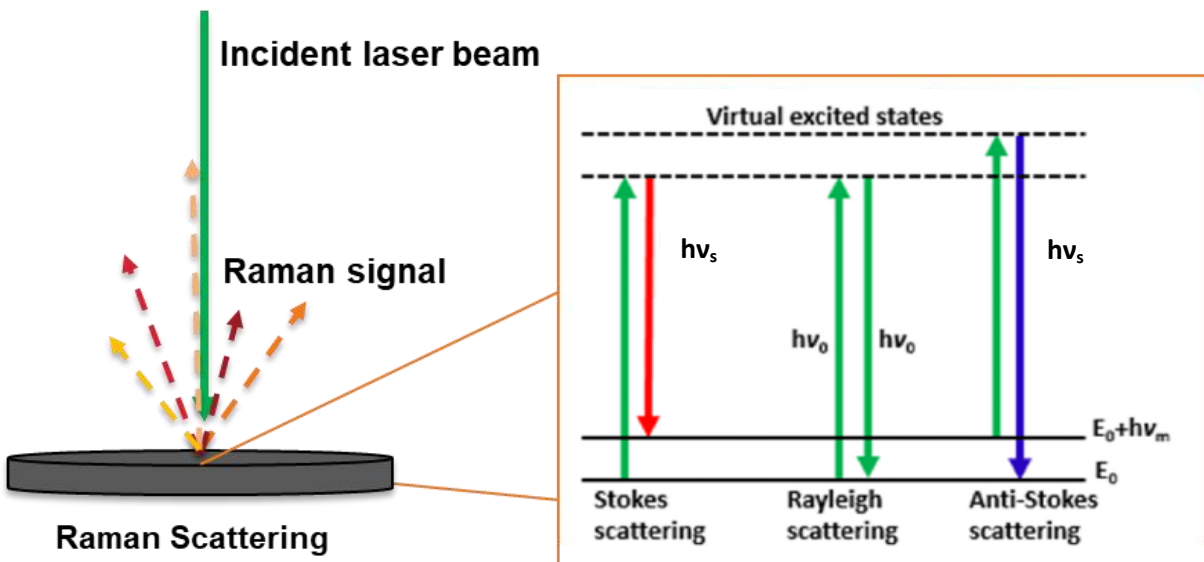


Figure 1: Diagram representing different forms of scattering. Left: A 532 nm green laser beam is incident upon the sample site where scattering occurs. A scattering signal consisting of different wavelengths is reemitted, with the signal at each of the wavelengths depending on the amount of energy lost to molecular vibrations. Right [1]: An energy diagram indicates the difference between Stokes and Anti-Stokes Raman scattering. Stokes scattering is much more common than Anti-Stokes scattering, and the reemitted light has lower or higher wavelength, respectively, than the original laser beam.

Raman scattering is further classified as Stokes and Anti-Stokes scattering. The absorption of an incident photon with energy $h\nu_0$ (note: this is not the absorption of the whole incident laser beam) is followed by the emission of a scattered photon with energy $h\nu_s$. Figure 1 shows different energy levels of the excited electronic state after absorption. The arrows pointing up depict laser energy absorbed, differing from the arrows pointing down, which show reemitted photon energy. Stokes scattering, which occurs much more frequently than Anti-Stokes scattering, arises after energy has been lost to molecular vibrations. In this situation, the reemitted photon has less energy than the initial photon. A lower-energy photon will oscillate at a lower frequency and therefore have a longer wavelength. Anti-Stokes scattering occurs when photons are reemitted with more energy than what was initially absorbed. In this case, the molecule is already vibrating and in an excited state. The energy from the excited state is added to the energy of the absorbed (pump) photon, so the reemitted photon is more energetic and therefore oscillates at a higher frequency (and has a shorter wavelength). The type of scattering occurring is depicted by the directions in which the Raman peaks are shifted – Stokes to the right of the origin with positive wavenumber shifts, and Anti-Stokes to the left with negative wavenumber shifts. In this experiment, Stokes scattering is considered (Figure 2). Had there been observations of leftward (negative) shifts of the signal wavenumber, they would have indicated Anti-Stokes scattering.

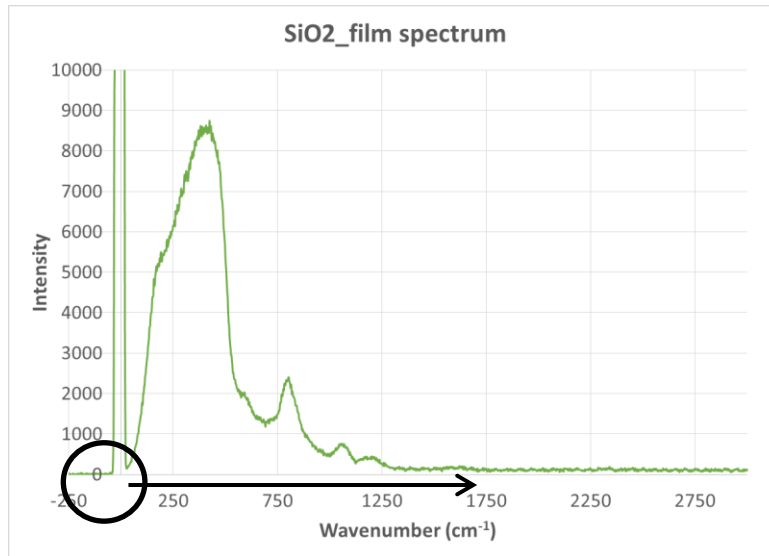


Figure 2: A neat (undamaged) silica film spectrum. The black circle indicates the origin at which zero wavenumber shift is located. The black arrow points to the rightward shift of the signal wavenumbers (i.e. Stokes scattering). In this and similar figures, “wavenumber” indicates wavenumber shift.

The main immediate purpose of this work is to better understand how damage forms. Most fundamentally, this work strives to answer the questions of how material (silica or hafnia) and its density change. Fused silica is supposed to be amorphous (as opposed to crystalline quartz), but previous research shows that silicon dioxide polymorphs (a solid material that can exist in more than one form or crystal structure) form at extreme conditions [2]. If polymorphs are determined to be present, then a following question would involve further research on which polymorphs (shistovite, coesite) form, why, and how. This information would be useful to learn about the conditions that exist during damage as certain polymorphs require a specific temperature or pressure to form. Micro-Raman spectroscopy is an alternative method to detect damage and provide information on how the material might be changing.

2. Background

In previous studies at the Laboratory for Laser Energetics (LLE), abnormal peaks were observed on a spectrum taken on a silica damage site. As can be seen in Figure 3, a strange spike is apparent at approximately 495 cm^{-1} , where other spectra slope down in a smooth curve.

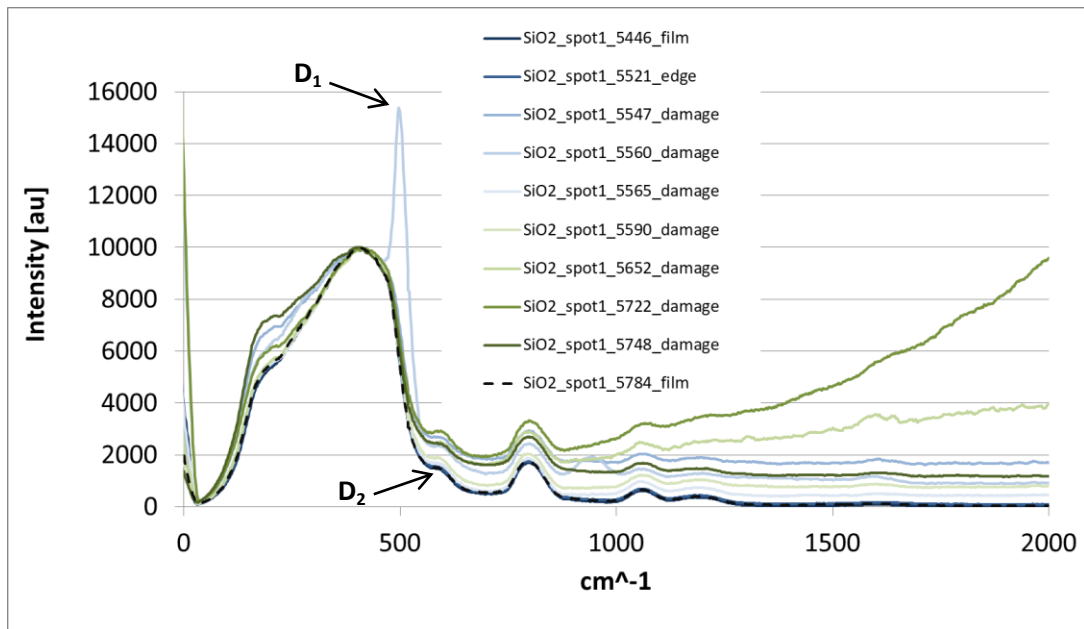


Figure 3: Graph depicting the abnormal peak on a spectrum taken from a silica damage site. Comparison with literature data identifies the peak as a defect, D_1 . The emerging peak to the right of it is identified as another defect, D_2 [3]. The dashed curve (for readability) and the dark blue curve are undamaged film spectra. Their close overlap with each other indicates that undamaged film spectra are reproducible. Other solid curves are damaged film spectra (previous data acquired by Dr. T. Kosci). The D_1 defect feature is not observed on other damage film spectra as it is a rare material modification detected at only that location.

To investigate these defects, spectra obtained at LLE were compared with data presented in the literature. It was determined that the peaks arise as a result of molecular defects. The spike at 495 cm^{-1} is identified as a defect, D_1 [3]. In Figure 3, emerging peaks at approximately 600 cm^{-1} consistently appear in each of the spectra produced. This defect feature also appears on the two undamaged film spectra in figure 3 because this feature is commonly occurring and is not a modification due to the laser pulse. This feature could be strengthened by laser irradiation.

According to data from the literature (see Figure 4), these peaks at 600 cm^{-1} are identified as a defect, D_2 [3]. However, unlike the distinct peaks presented in Figure 4, the D_2 peak in Figure 3 is less obvious and is more characteristically similar to a knee feature than a Raman defect peak. Yet, its location and consistent appearance suggest that it is a defect peak riding on photoluminescence signals. Photoluminescence (PL) is also the reemission of absorbed light at lower wavelengths, but the mechanism of energy loss differs from Raman processes. After light has been absorbed by an irradiated sample and molecules enter a higher (excitation) electronic state, PL is the emission of light that occurs when photons are released as molecules return to a lower energy level. PL signals can often mask the Raman signal.

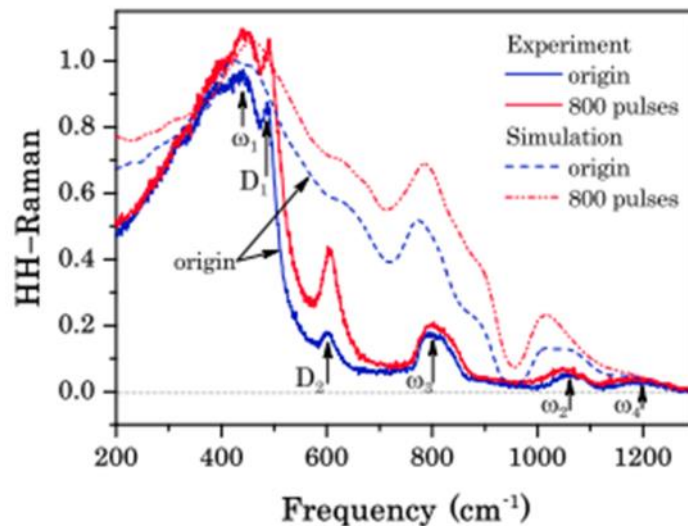


Figure 4: Identification of defect peaks. This graph, published by Shcheblanov [3], identifies D_1 and D_2 peaks along with other reference wavenumbers that are also found in LLE data (Figure 3) and produces evidence that the sharp peak (D_1) at 495 cm^{-1} is reproducible.

According to the literature, the D_1 and D_2 Raman defect spectra are due to the symmetric stretch of four- and threefold rings in the structure of vitreous silica [3, 4]. It is probable that the damage in silica results in a laser-induced densification [3]. Due to the similarities of traits

presented on the spectra, an analogous process could be inferred about the laser-induced damage spots produced at LLE.

3. Experimental Setup

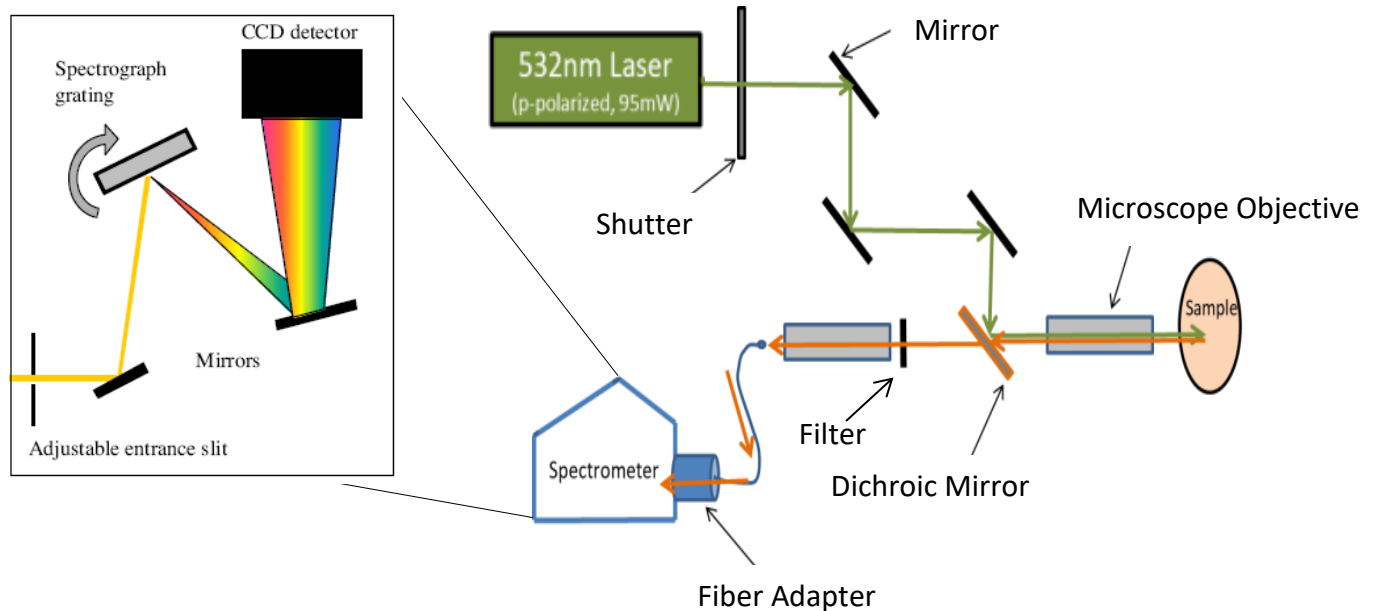


Figure 5: Experimental setup. The path that the laser beam takes from the laser source to the thin film sample is depicted by the green arrows. The path of the reemitted signal from the sample is represented by the orange arrows.

To conduct this research, a Laser Quantum GEM532 continuous laser (p-polarized, 95 mW) is used to probe silica and hafnia sample damage sites. As shown in Figure 5, the laser beam passes through a shutter and is then aligned by three consecutive mirrors positioned at 45 degrees. Reflected off the third mirror, the 532 nm laser beam hits a Razor Edge 532 dichroic mirror, designed for maximum reflection of 532 nm light at a 45-degree angle of incidence. (All other wavelengths are transmitted.) The dichroic mirror reflects green light and directs the laser beam to its target site on the sample. The laser beam is focused by a Mitutoyo WE835003118 M Plan Apo microscope objective onto specific locations on damage sites.

The laser beam is focused on silica damage sites of approximately 200 microns or hafnia damage sites ranging from approximately 70 to 400 microns. Upon radiation, the Raman scattering is collected by the same microscope objective and passes back through the dichroic mirror. Since the Raman scattering consists of wavelengths other than 532 nm, it is transmitted through the dichroic mirror. Unfortunately, this mirror does not filter out the 532 nm light entirely. Hence, a Razor Edge 532 filter is installed to filter out as much of the 532 nm wavelength from the scattering signal as possible to prevent overwhelming the Raman spectra with a strong green laser beam signal.

After the filter, the laser beam passes through an Opto Sigma, PAL-10-A, J11406689, 10x Plan, microscope objective, which focuses the scattering signal into a fiber optic. The light enters a fiber adapter where two lenses collimate the light and then properly focus the rays onto the 100-micron entrance slit of the Horiba iHR320 spectrometer. In the Horiba spectrometer, the signal is dispersed by a 600 lines/mm diffraction grating. The dispersed light is projected onto the pixels of a charge-couple device (CCD) detector to capture the signal spectrum.

4. Results

4.1 Silica Laser-Induced Damage Spots and Site Mapping

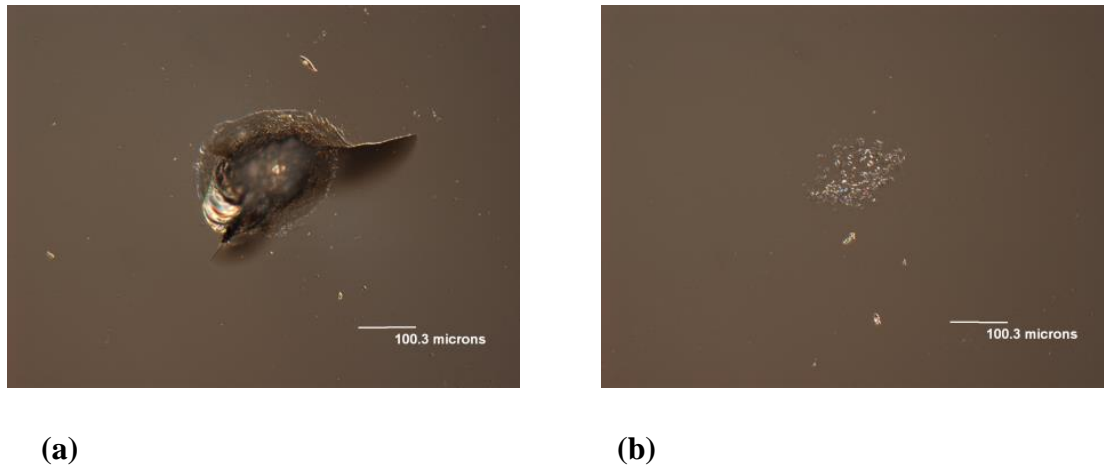


Figure 6: (a) Damage spot 15 on the silica sample, damaged under high fluence. (b) Damage spot 21 on the silica sample, damaged under low fluence.

Using a Leica microscope, damage sites on both silica and hafnia samples were mapped out. Under the microscope, consecutive damage sites are in lines, increasing in visibility from one end to the other. This pattern is evidence that these sites were created with increasing laser fluences. Sites were distinguished from dust on the samples by their rounded shapes, organized formation for silica sites, and coloration for hafnia sites. Using one easily identifiable spot on the samples as the origin, the relative positions of each site were noted. Each damage site was labeled with a number and images similar to Figure 6a and 6b were captured.

Sample damage spots are produced with high and low fluences as well as with different testing protocols, including 1-on-1 and N-on-1 testing [5]. 1-on-1 testing involves irradiating a test site once at a specific laser fluence. N-on-1 testing involves irradiating a test site multiple times, each time with an increased fluence, until damage is created. Under the microscope, the sites are distinguished by their damage widths and features. Certain damage spots are observed with cracks that extend beyond the edges (Figure 6a). Some damage spots created under higher

fluences are observed to contain melted material, which creates depth to the damage site. Figure 6b shows a light damage spot with low material modification, which was created using a low fluence.

4.2 Silica Data Spectral Analysis

To better understand the unique characteristics present in the spectra of damaged spots, undamaged, or “neat,” silica films were probed and compared. As depicted in Figure 7, it is evident that the neat films are characteristically similar. Normalized data result in nearly identical spectra that overlap each other. This confirms the hypothesis that neat silica films will have a similar molecular composition. Slight signal intensity discrepancies are noted at approximately 200 cm^{-1} and from 550 cm^{-1} to 1050 cm^{-1} , which are indicated by the red circles in Figure 7. These discrepancies are hypothesized to be caused by slightly different interactions of the sample surface with its environment, which are probably insignificant in the study of laser-induced damage.

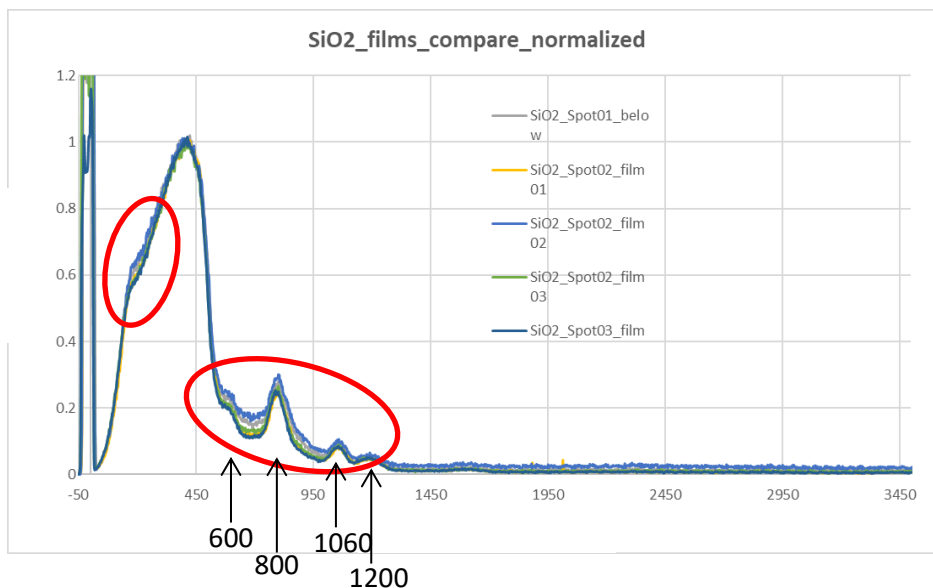


Figure 7: Comparison of normalized neat film spectra probed in various areas on the silica sample. Subtle differences in spectral feature intensities are observed (indicated by the red circles).

To identify material modifications on silica thin films resulting from laser-induced damage, spectra from neat films were compared with damage site spectra. Two damage spots on the silica sample were selected and probed at various positions within each spot. No additional peaks were noted in the damage sites to indicate defects. Looking at the spectra from damaged spot 02 shown in Figure 8, it is observed that while the main characteristics of the Raman signal, such as the Raman peaks prior to 1750 cm^{-1} , are present in each spectrum, the intensities of the spectra taken at the same location on spot 02 differ largely within the range from approximately 550 cm^{-1} to 7000 cm^{-1} . In Figure 8, the differences in magnitude are obvious when the spectra from two damaged sites (try1 and try75) are compared with the neat film spectrum (flat green curve). These variations likely arise due to PL resulting from the laser irradiation.

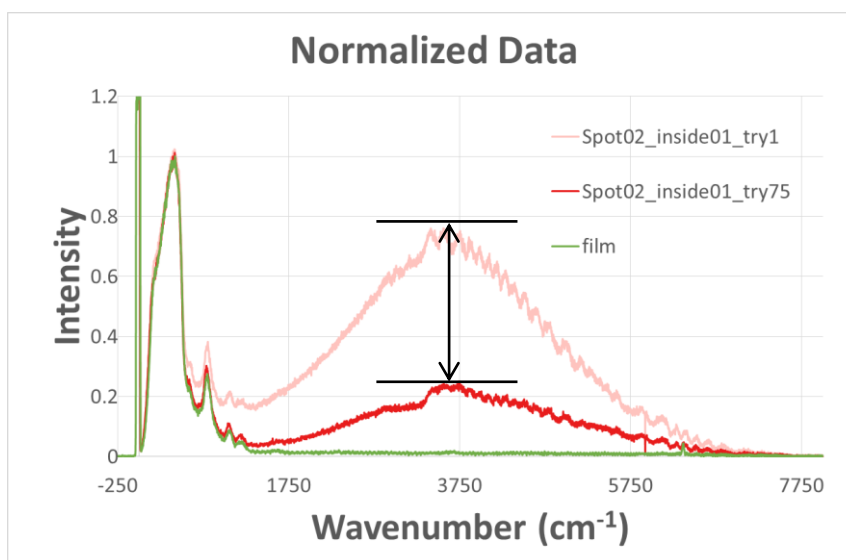


Figure 8: Decay of silica PL signals. The pink curve represents data collected from the first laser irradiation at spot 02. The red curve represents data collected from the last laser irradiation (the seventy-fifth spectrum) at the same location in spot 02. The spectra of damage spot 02 are normalized to the main Raman peak to facilitate data comparison and to account for the effect of PL. The black arrow outlines the decrease in PL in a single position in silica damage spot 02. The green curve is a neat film spectrum.

The magnitude of the PL was investigated as a function of time. A total of seventy-five spectra were collected from spot 02 over three days, with a total of approximately six hours of

irradiation to study PL decay. Each day, the damage site in spot 02 was probed with an acquisition time of ten seconds for each spectrum. On the first day, the site was probed consecutively for nearly one hour. The setting was left exactly the same to continue laser irradiation on the second day for approximately four hours of acquiring spectra with the laser turned off between each day. The same process was repeated the third day to acquire the remaining spectra. There were twenty-minute rest intervals and five-minute rest intervals in between each acquisition on the second and third days, respectively. In Figure 8, the pink and red spectra represent the investigated net decay over time. While the intensity at that particular sample position continued to decay, its rate of decay was minimal compared to the first few spectra that were taken. The changing signal intensities could be due to prolonged laser irradiation (exposure) over the duration of acquiring the 75 spectra as well as reaction to the environment. When comparing all spectra taken from silica damage spots, the main Raman features are all present and similar. Yet, the levels of PL appear to vary from one position within the damage site to another. These data suggest that somewhat different PL signatures are produced by laser-induced damage at various sites. Note that aside from PL signals in the spectra, the Raman features (see Figure 8 at $<1750\text{ cm}^{-1}$) are all relatively uniform without notable abnormal features. In three inspected silica damage sites, though various positions were probed and analyzed, a strong D_1 ($\sim 495\text{ cm}^{-1}$) or D_2 ($\sim 600\text{ cm}^{-1}$) peak was not found other than the identified D_1 peak in figure 3, underscoring their rarity in being observed.

4.3 Hafnia Laser-Induced Damage Spots

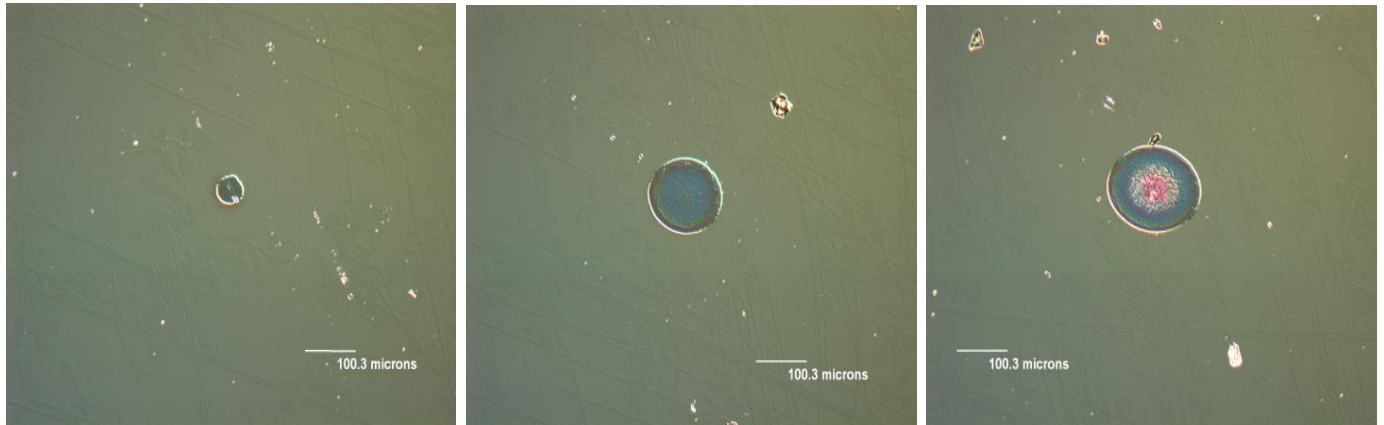


Figure 9: A series of hafnia damage sites created with increasing fluence, starting from the leftmost image to the right. The images depict spots 20, 21, and 22, respectively.

Overall, hafnia damage spots have greater variability in their sizes compared to those of silica. Differences due to fluence levels in addition to other test protocols are distinguishable through the damage areas, which are depicted in Figure 9. The most notable difference is the varying sizes of each site. Considering all hafnia damage sites, they range from approximately 30 microns to 400 microns in width (Figure 9 depicts a range of 30 to 200 microns).

4.4 Hafnia Data Spectral Analysis

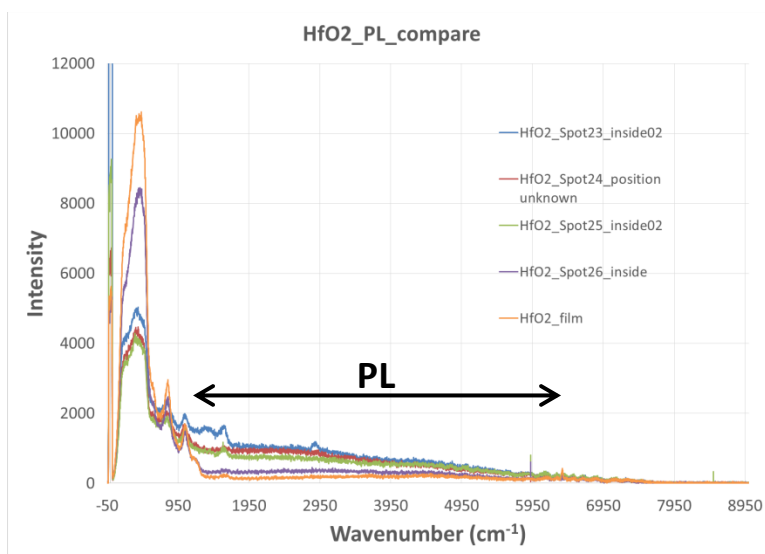


Figure 10: A study of hafnia PL signals. Damaged site PL spectra are all relatively low in intensity, yet greater in intensity compared to the film spectrum and span approximately from 1000 cm^{-1} to 6000 cm^{-1} .

Most spectra produced from damaged sites show similar features, with relatively low intensity PL signals that span from 1000 to 6000 cm^{-1} (Figure 10). Note that the spectrum for spot 23 (blue curve) has two unusual features at ~ 1500 and 2900 cm^{-1} . These peaks have not yet been identified and could yield interesting information.

An unusual signal behavior is observed in spectra from spot 29 shown in Figure 11. The first spectrum taken at spot 29 on the first day shows a very large PL signal. With a 10-second acquisition time for each spectrum, this same position was again probed over the course of three days in half-hour intervals for a total of six hours. The laser was turned off at the end of each day while the setup was kept exactly the same to continue probing at that position the next day. It was observed that the first spectrum taken at the spot each day increased in intensity slightly above the last spectrum taken from the previous day. The final spectra of each day all eventually declined to about the same level of intensity. The decreasing rate of PL signal decline is presented in Figure 11.

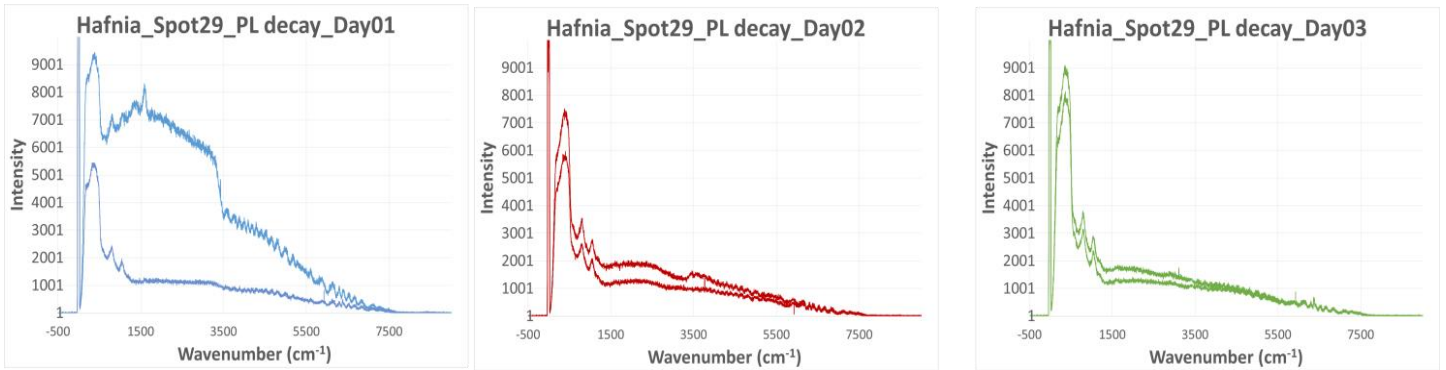


Figure 11: Signal intensity decay of an unusually large signal at spot 29 of the hafnia sample. This figure illustrates the decreasing signal intensity at a slowing rate. The spectra in each graph represent the differences in intensity between the first and last spectra obtained in a day.

To study the PL signal decrease, a comparison between data taken on the three separate days was created (Figure 12). It is noted that each PL signal eventually decayed to approximately the same intensity level, which reflects consistent material modification at that particular damage spot. However, through this comparison, it is observed that although PL signals have decayed, the relative intensity of the Raman signal appears to have increased over time, though the exact reason for this remains unclear.

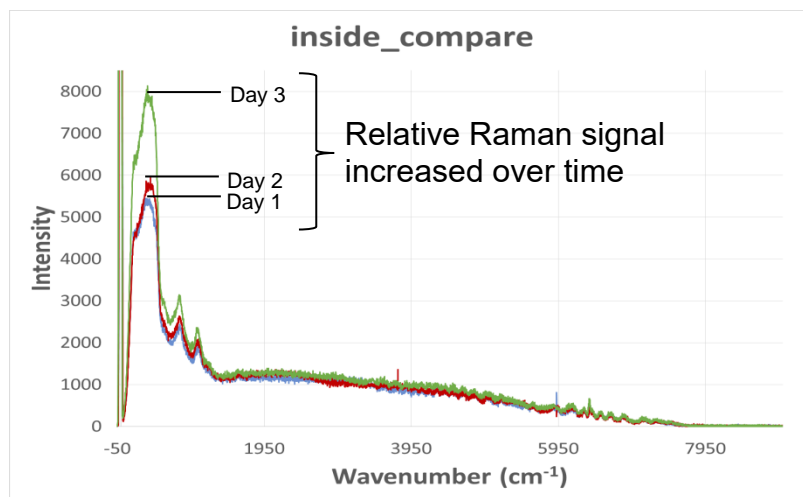


Figure 12: Comparison of the last spectra taken from spot 29 from day 01, day 02, and day 03 of observations (the three lower spectra from Figure 11).

To compare the differences between hafnia damage test sites created with high versus low fluence, damage sites from both were probed. The damage spots representing high fluence are spots 24, 25, 26, and 29 [Figure 13(a)]. The damage spot representing low fluence is spot N1, created with an N-on-1 test, with data taken from various locations within the site [Figure 13(b)]. In spot N1, similar spectra are reproduced repeatedly, with spectra closely overlapping each other. This suggests that little material change occurred in this spot despite the slight damage. Apparent in Figure 13, the spectra acquired from high fluence damage spots demonstrate significantly larger intensity levels whereas the damage test spots created by N-on-1 tests at low fluence depict low intensity levels and relatively little deviation from the neat film spectrum.

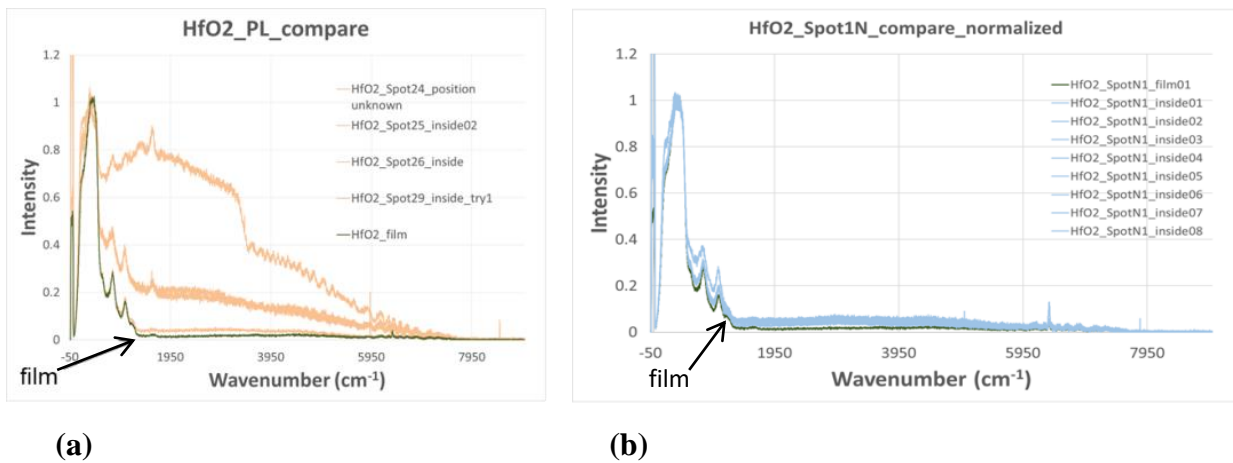


Figure 13: Comparison of signal intensity levels between the spectra of low and high fluence laser-induced damage in the hafnia sample. Figure 13(a) depicts the spectra of a high fluence damage site, which shows high intensity signals with the exception of the bottom yellow curve (spot 26), which is similar to the film spectrum. Figure 13(b) represents the spectra of a low fluence damage site, which shows low intensity signals, resembling the neat film spectrum.

4.5 Comparing Silica and Hafnia Data Spectra

When comparing silica data with hafnia data, certain features are highlighted. For instance, neat film spectra from both samples were compared to observe potential differences between undamaged films. Normalized data (Figure 14) show that while silica neat film spectra are fairly reproducible, with flat curves consistently overlapping each other, hafnia neat film spectra suggest some PL that spans from approximately 400 cm^{-1} to 7000 cm^{-1} . When hafnia neat film spectra are compared to hafnia damage site spectra, they appear to be flat. However, when the spectra from both samples are placed together on the same graph, as in Figure 14, the PL signals become distinct. Potentially, the hafnia film spectra could be riding on a small PL signal, leading to raised features. When normalized to the main Raman peak, the two subsequent hafnia Raman peaks at 810 and 1065 cm^{-1} are also raised in comparison to those of silica.

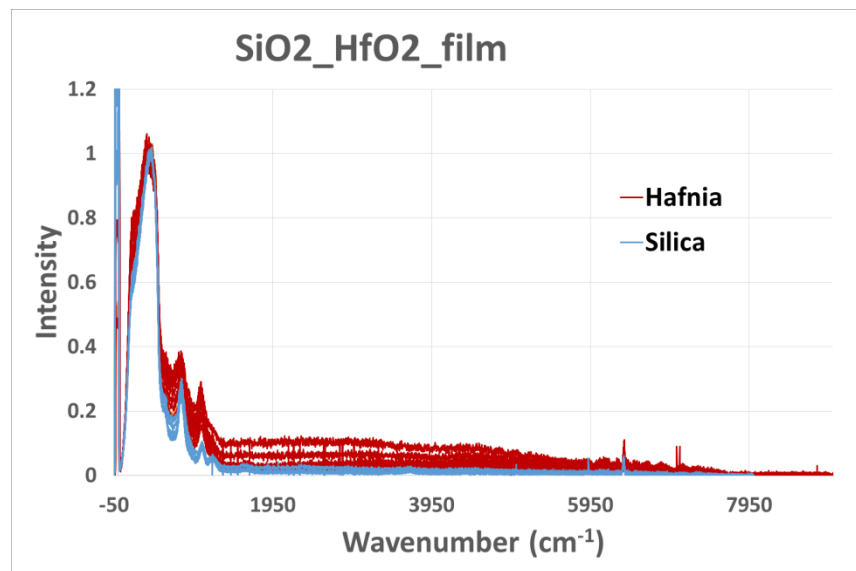


Figure 14: Comparison of silica and hafnia neat film spectra. The PL signals in the hafnia data are highlighted when placed together with the silica data.

Results from the spectral comparison shown in Figure 15 reveal two additional features that are observed in silica spectra but not hafnia spectra. These two features, a knee and a peak,

are observed in silica neat film spectra as well as inside damaged spots. The knee feature is visible around 600 cm^{-1} , and the peak is visible around 1200 cm^{-1} .

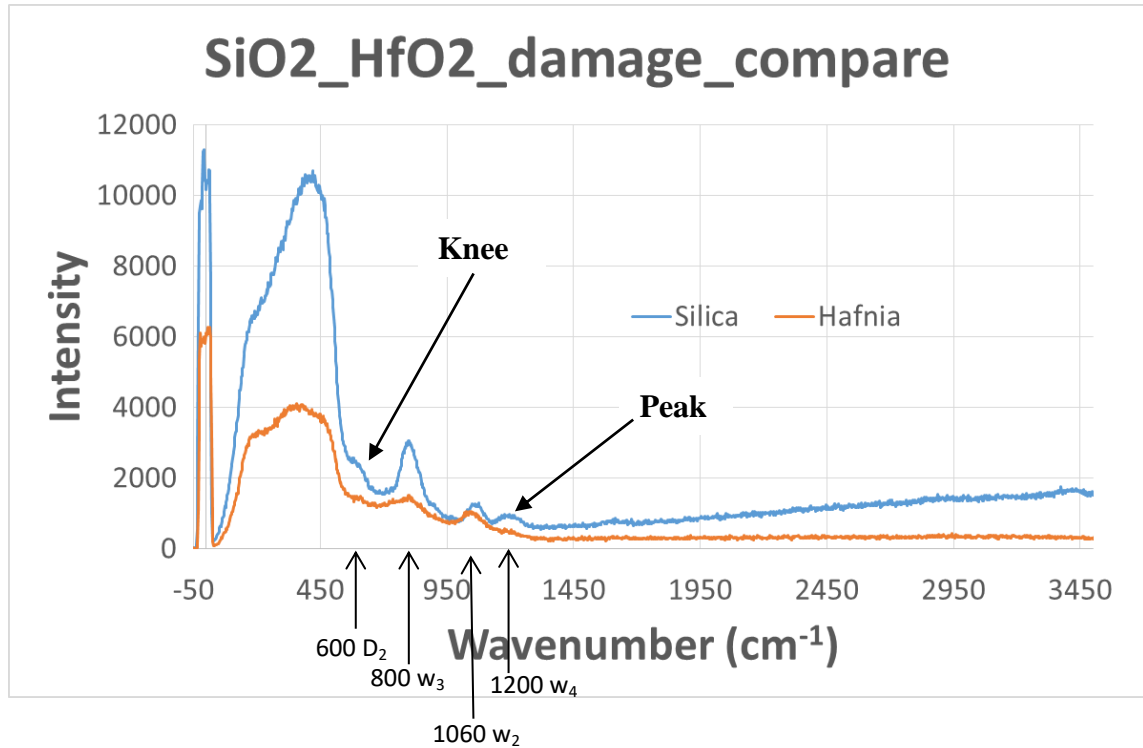


Figure 15: Comparison of silica and hafnia damaged site spectra. The black arrows point to additional knee and peak features that are not visibly observed in hafnia spectra. Note that the four silica peaks (D_2 , w_3 , w_2 , and w_4) match those in figure 4 exactly.

From Figure 15 it appears that the knee and peak are unique characteristics of silica. However, a close-up study of the curves reveals emerging knee and peak features on hafnia spectra as well, though much weaker. This observation was made on nearly all hafnia spectra, be it on neat film or damage sites. These spectral features are clearly identifiable in some hafnia spectra while barely visible in most others. A proposed explanation is that the visibility of these spectral features depends on the proximity of the excitation laser to the silica substrate, which is used for both film samples. To test this hypothesis, a depth study was conducted on the hafnia

sample. This involved probing the sample in the air above the target site, on the surface, and beyond the surface.

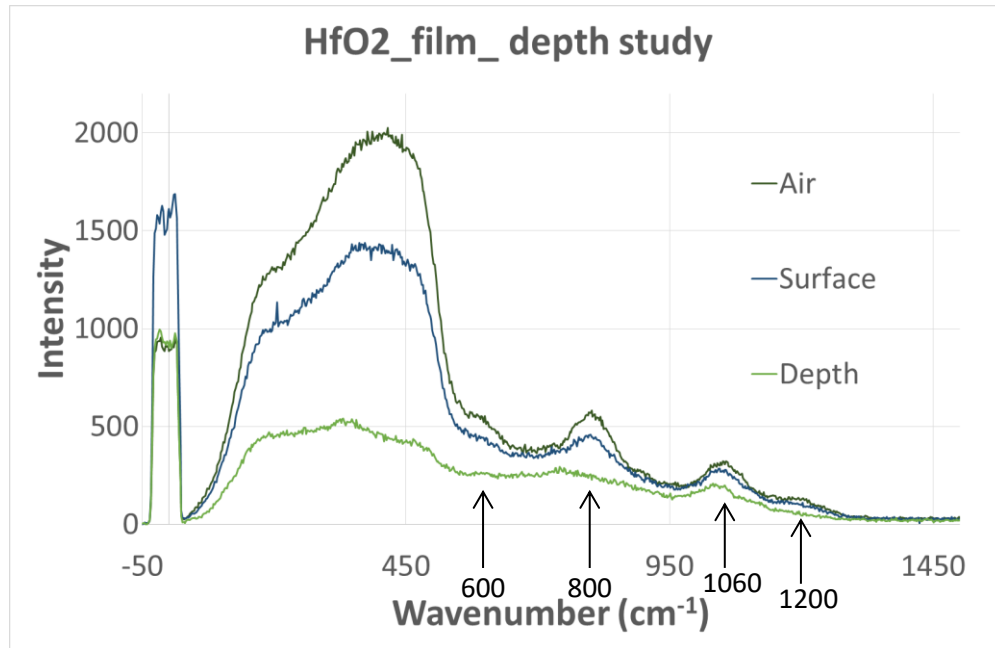


Figure 16: Comparison of depth study spectra. The three representative spectra show resulting data taken from air (above), surface (on the same dimension as the sample), and depth (past the surface). The specific measurements for the spectra in this figure use the surface as the standard position. The focal point of the excitation laser beam is moved out 0.105 mm above the surface and moved 0.145 mm past the surface.

Depth study results suggest that the visibility of the spectral features at 600 and 1200 cm^{-1} can be affected by the position of the excitation source. As the laser beam probes below the surface of the sample, the knee and peak features are no longer visible on the spectra. As seen in Figure 16, the lowest-intensity spectrum (probed beneath the surface) has no knee at 600 cm^{-1} and no peak at 1200 cm^{-1} , whereas the top two spectra, acquired at and above the sample surface, show both features at the indicated wavenumbers. This observation is repeatedly seen on other spectra, which are taken from other positions with varying depths. This may indicate different material compositions (or interactions) beneath the surface of damage sites.

Summary

Micro-Raman spectroscopy was used to identify material modifications in silica and hafnia laser-induced damage sites. By probing the damage sites with an incident laser beam, spectra with identifying characteristics were produced. These spectra allow for comparisons between damaged and undamaged film materials and have identified transient features, such as the disappearing hafnia features. Raman spectra of silica and hafnia proved to be similar, but not identical. The main difference between silica and hafnia lies in their signal intensity levels. Hafnia spectra tend to have higher PL signals, which tend to obscure some spectral features more than in silica spectra. Damaged and undamaged spectra in silica portray similar characteristics, and the previously observed rare D_1 and D_2 features at 495 cm^{-1} and 600 cm^{-1} , respectively, were not found in any new spectra. The main Raman peaks are present in all spectra, though PL signals are evident in most damaged spectra. A depth study showed that the distance above or below the sample surface at which the sample is probed affects the signal intensity. Research on material modifications using micro-Raman spectroscopy could be applied to improve understanding of the laser-damage process and future manufacturing of laser thin film coatings.

Acknowledgements

I would like to thank Dr. Tanya Kosc, my advisor, for her endless help and support throughout this project. Her patience during discussions offered invaluable insight and inspiration. Thank you to Dr. Stephen Craxton, who offered me this opportunity to learn about micro-Raman spectroscopy. I would also like to thank Dr. Stavros Demos and Mr. Alexei Kozlov for giving me much appreciated suggestions on my project. Many thanks to the Optical Material

Technologies group members for making it possible for me to spend extensive time working with lasers in the lab.

References

- [1] Lohumi, Santosh & Kim, Moon Seok & Qin, Jianwei & Cho, Byoung-Kwan. (2017). Raman imaging from microscopy to macroscopy: Quality and safety control of biological materials. *TrAC Trends in Analytical Chemistry*. 93. 10.1016/j.trac.2017.06.002.
- [2] K. J. Kingma, R. J. Hemley; Raman spectroscopic study of microcrystalline silica. *American Mineralogist* ; 79 (3-4): 269–273.
- [3] N. S. Shcheblanov, M. E. Povarnitsyn, K. N. Mishchik, and A. Tanguy; Raman spectroscopy of femtosecond multipulse irradiation of vitreous silica: Experiment and simulation. *Phys. Rev. B* 97, 054106 (2018)
- [4] A. E. Geissberger, F. L. Galeener; Raman studies of vitreous SiO₂ versus fictive temperature. *Phys. Rev. B* 28, 3266 (1983)
- [5] A. A. Kozlov *et al.* Study of the picosecond laser damage in HFO₂/SiO₂-based thin-film coatings in vacuum. *Proc. SPIE* 10014, (100141Y (2017)).